

Simulation Tools, VT23

Report on Project 1

Salvador Castagnino, Theo Koppenhöfer

January 27, 2023

Introduction

The Benchmark

In the following we use the model of a pendulum attached to a rod which is elastic in the radial direction as described in Task 1. The situation is depicted in figure 1.

In particular our ODE is given by

$$\begin{bmatrix} y_1 \\ y_2 \\ y_3 \\ y_4 \end{bmatrix}' = \begin{bmatrix} y_3 \\ y_4 \\ -y_1 \lambda(y_1, y_2) \\ -y_2 \lambda(y_1, y_2) - 1 \end{bmatrix}$$

with

$$\lambda(y_1, y_2) = k \frac{\|(y_1, y_2)\| - 1}{\|(y_1, y_2)\|}.$$

The plot of a numerical solution to this problem for $k = 1$ can be seen in figures 2 and 3.

We can calculate the potential, kinetic and approximate the elastic energy with the formulas

$$E_{\text{pot}} = 1 + y_2 \quad E_{\text{kin}} = \frac{\|(y_3, y_4)\|^2}{2} \quad E_{\text{elast}} = k \frac{(\|(y_1, y_2)\| - 1)^2}{2}.$$

Adding these up we get the approximate total energy

$$E_{\text{tot}} = E_{\text{pot}} + E_{\text{kin}} + E_{\text{elast}}.$$

We expect the approximate total energy to be constant which indeed can be seen in Figure 5. Because of this property we can use the relative variation of the approximate total energy as an index meas implement

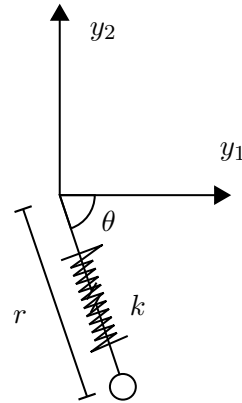


Figure 1: The pendulum

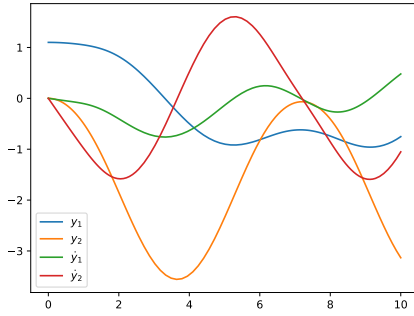


Figure 2: State in dependence of time.

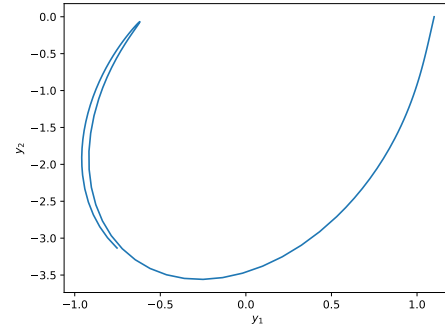


Figure 3: Path traced out by pendulum.

```
import numpy as np
instability_index = (np.max(total_energy) - np.min(total_energy)) \
                    / np.mean(total_energy)
```

In the ideal world this index almost vanishes.

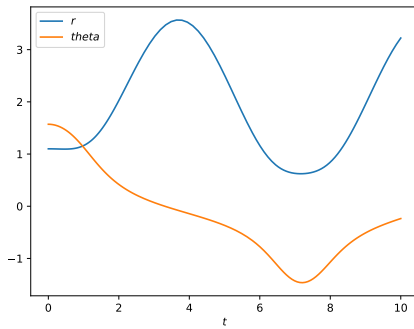


Figure 4: Polar coordinates.

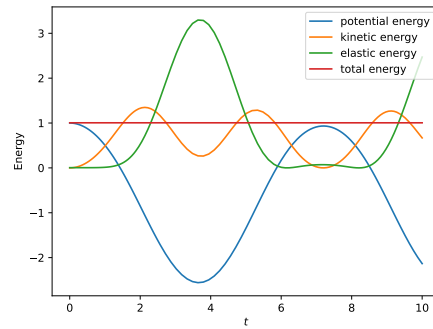


Figure 5: Energy plot

Testing CVODE

A first test series

In the first specific test of CVODE we solve our toy problem for increasing k . Hereby we switch between the BDF and Adam-Moultons discretisation method. We also vary the `maxorder` parameter for both methods. A higher k reflects a problem which is more stiff. As a stiff problem requires finer steps the number of steps `nsteps` increases as k increases which is what can be seen in figure 6. As the number of function evaluations per stepsize `nfcns/nsteps` hovers slightly above 1 for all methods (c.f. figure 8) the number of function evaluations increase correspondingly as can be seen in figure 7. There

is however a difference in how many steps each method needs. The BDF-method requires in general more steps than the Adams-Moulton method. And the general trend is that the number of steps increases as `maxord` is reduced.

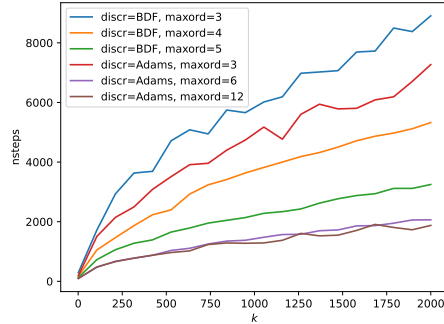


Figure 6: `nsteps` in relation to the parameter k .

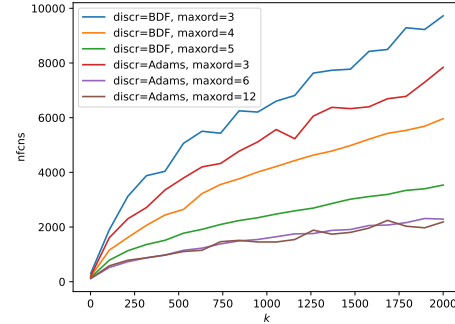


Figure 7: `nfuncs` in relation to the parameter k .

From figure 9 it can be seen that the number of jacobian evaluations stays roughly constant and happens roughly every 5th step. The number `nerrfails/steps` stays roughly constant in dependence of k though the general tendency is that it is smaller the lower `maxord` is set. This makes sense because a lower `maxord` means there are fewer possibilities to change the method order to and hence fewer changes of order. In figure 11 we see a difference in how much the methods obey the principles of energy conservation. One can see that for growing k the result tends to be further away from physical reality. Once again the methods with higher `maxord` do better with the exception of the BDF method where for some reason a `maxord` of 4 performs best.

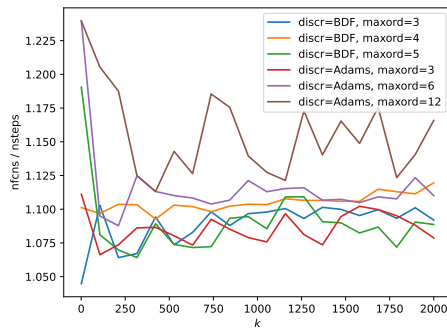


Figure 8: `nfuncs/nsteps` in relation to the parameter k .

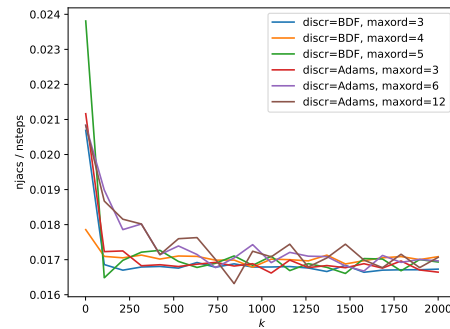


Figure 9: `njacs/nsteps` in relation to the parameter k .

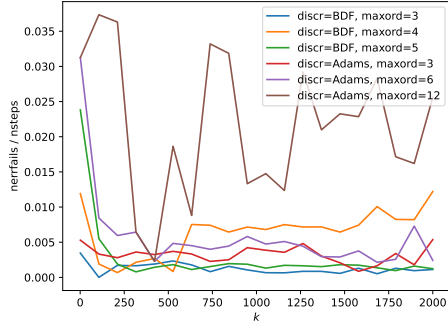


Figure 10: $\text{nerrfails}/\text{nsteps}$ in relation to the parameter k .

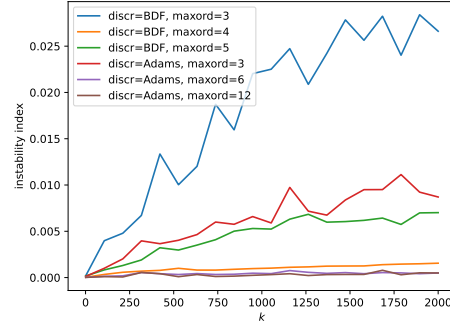


Figure 11: instability index in relation to the parameter k .

Testing the parameter rtol

We now test the influence of the parameter rtol on the methods BDF and Adams-Moulton. For this we set $k = 10^3$ and keep all other parameters on their default values. The results can be seen in figures 12 to 16. We note that as rtol increases the number of steps decreases (c.f. figure 12). If one compares figures the instability index for $k \approx 10^3$ in figure 11 with the instability index in figure 16 one sees that setting the rtol parameter makes the result significantly worse.

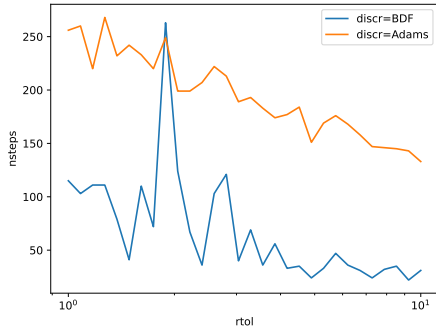


Figure 12: nsteps in relation to the parameter rtol .

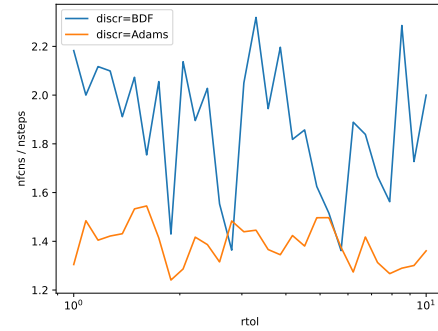


Figure 13: $\text{nfcns}/\text{nsteps}$ in relation to the parameter rtol .

Testing the parameter atol

If we test the atol parameter on the Adams and Newton method analogously to the test of the rtol parameter we once again get an instability index that is significantly above the value for the method in which we did not specify this value as can be seen in Figure 17. In either case we observe that fixing the tolerance seems to come at the cost

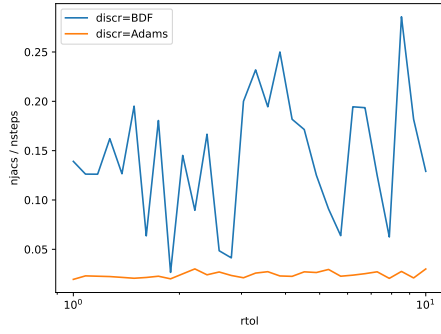


Figure 14: $\text{njacs}/\text{nsteps}$ in relation to the parameter rtol .

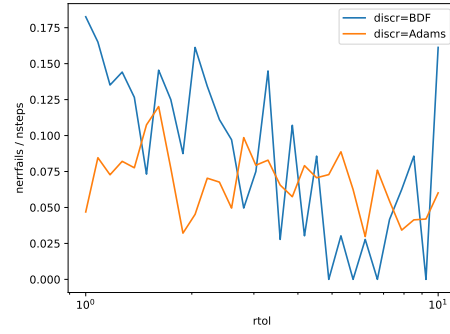


Figure 15: $\text{nerrfails}/\text{nsteps}$ in relation to the parameter rtol .

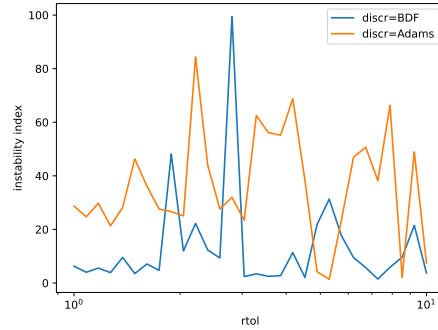


Figure 16: instability index in relation to the parameter rtol .

of energy conversation as can be seen in the Figures 18 and 19.

References

- [1] Backward differentiation formula. *Estimation lemma* — *Wikipedia, The Free Encyclopedia*. Online; accessed 27-January-2023. 2022. URL: https://en.wikipedia.org/wiki/Backward_differentiation_formula.
- [2] Peter Deuffhard and Folkmar Bornemann. *Numerische Mathematik 2*. revised. de Gruyter Lehrbuch. [de Gruyter Textbook]. Gewöhnliche Differentialgleichungen. [Ordinary differential equations]. Walter de Gruyter & Co., Berlin, 2008, pp. xii+499. ISBN: 978-3-11-020356-1.

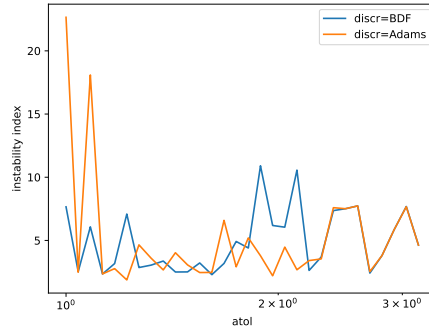


Figure 17: instability index in relation to the parameter $atol$.

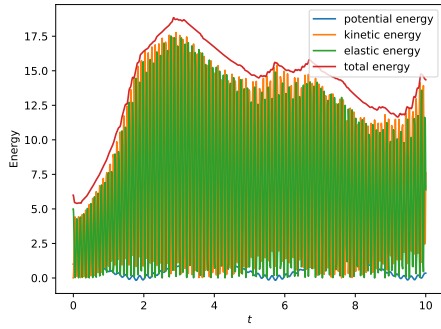


Figure 18: Energy plot for $k = 10^3$ with $atol = 1E-2$.

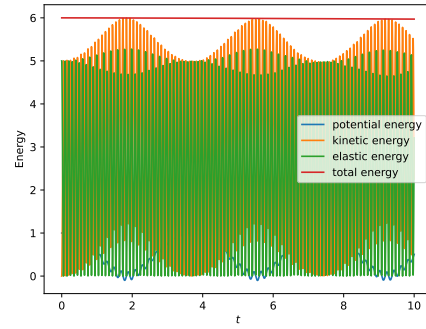


Figure 19: Energy plot for $k = 10^3$.

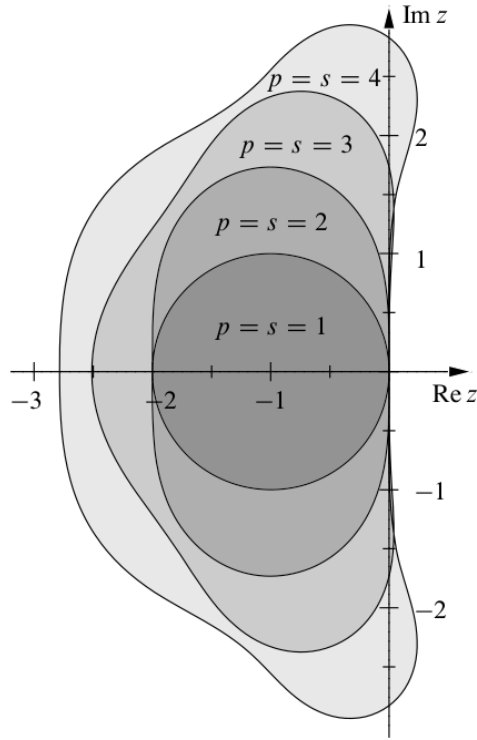


Figure 20: Stability regions of the Runge-Kutta-methods, taken from [2][p.238]

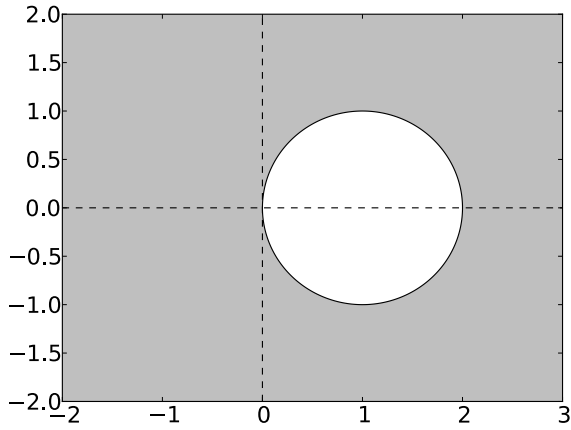


Figure 21: Stability region for BDF1, taken from [1]

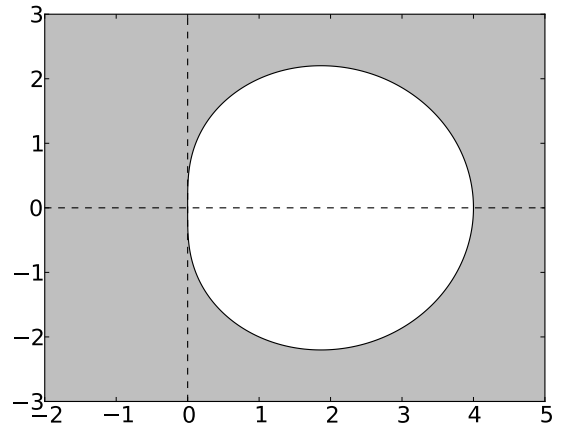


Figure 22: Stability region for BDF2, taken from [1]

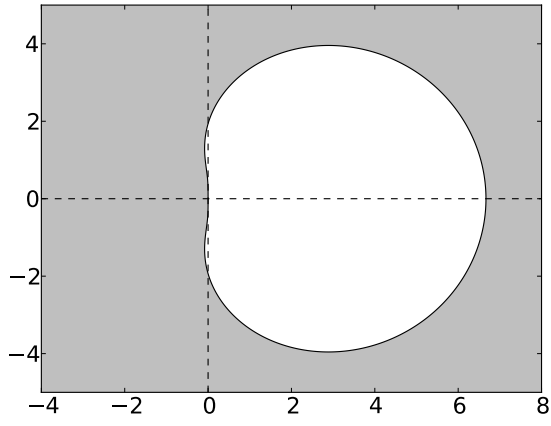


Figure 23: Stability region for BDF3,
taken from [1]

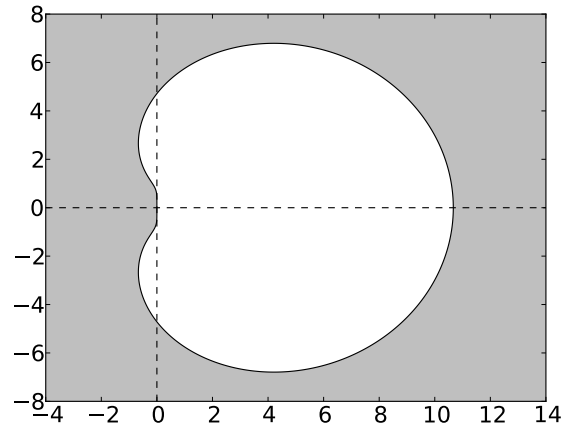


Figure 24: Stability region for BDF4,
taken from [1]

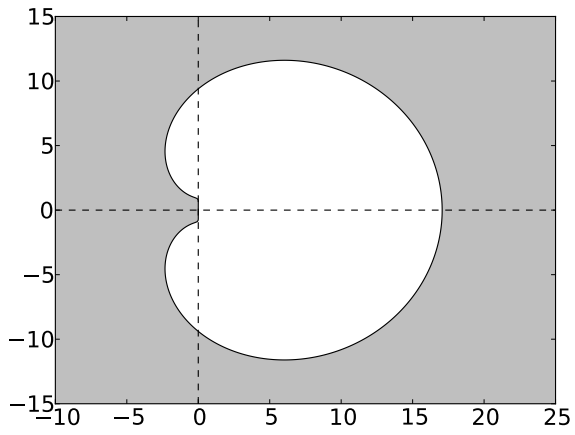


Figure 25: Stability region for BDF5,
taken from [1]

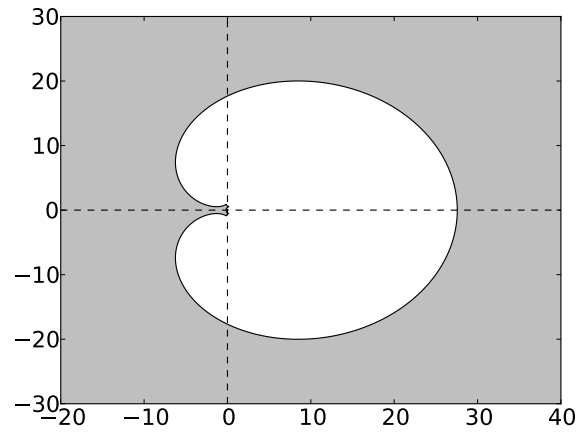


Figure 26: Stability region for BDF6,
taken from [1]